term must be added to Eq. (30) to subtract this portion of the radiative energy. Also, the collisional mass production term must be removed from the right side of Eq. (30). In the bound-free radiative processes, most of the radiation absorbed or emitted affects the zero point energy of the gas through the production or destruction of ionized or dissociated species. If the quantity of radiation absorbed or emitted in the bound-free processes is relatively small, the zero point energy could be removed from Eq. (31) without adding the correction term to Eq. (30). However, as the bound-free processes become more significant, this could result in unrealistically large electron/electronic temperatures. In this case, the zero point energy should be included in Eq. (31). In order to properly include the influence of this term, however, it is also necessary to add the effects of radiative transfer on the chemical production of each species as given by Eq. (16).

References

[1]Carlson, L. A., and Gally, T. A., "Nonequilibrium Chemical and Radiation Coupling Phenomena in AOTV Flowfields," AIAA Paper 91-0569, Jan. 1991.

[2]Lee, J. H., "Basic Governing Equations for the Flight Regimes of Aeroassisted Orbital Transfer Vehicles," AIAA Paper 84-1729, June 1984.

[3]Gnoffo, P. A., Gupta, R. N., and Shinn, J. L., "Conservation Equations and Physical Models for Hypersonic Air Flows in Thermal and Chemical Nonequilibrium," NASA TP 2867, Feb. 1989.

[4]Stanley, S. A., and Carlson, L. A., "Effects of Shock Wave Precursors Ahead of Hypersonic Entry Vehicles," *Journal of Spacecraft and Rockets*, Vol. 29, No. 2, 1992, pp. 190–197.

[5]Carlson, L. A., "Radiative Transfer, Chemical Nonequilibrium, and Two-Temperature Effects Behind a Reflected Shock Wave in Nitrogen," Ph.D. Dissertation, Ohio State Univ., Columbus, OH, 1969.

[6]Chapman, S., and Cowling, T. G., *The Mathematical Theory of Non-Uniform Gases*, 3rd ed., Cambridge Univ. Press, New York, 1970, p. 48.

[7]Carlson, L. A., and Gally, T. A., "Effect of Electron Temperature and Impact Ionization on Martian Return AOTV Flowfields," *Journal of Thermophysics and Heat Transfer*, Vol. 5, No. 1, 1991, pp. 9–20.

[8]Vincenti, W. G., and Kruger, C. H., Jr., *Introduction to Physical Gas Dynamics*, Kriger, Malabar, FL, 1986, p. 458.

Magnetized Plasma Flow over an Insulator at High Magnetic Reynolds Number

J. M. G. Chanty*

Massachusetts Institute of Technology, Cambridge, Massachusetts 02139

I. Introduction

ALTHOUGH magnetohydrodynamic (MHD) boundary layers have been the subject of considerable study,[1–5] little has been published on the physics of highly magnetized, high Reynolds number flows. The work presented here is an analysis of the self-similar solution to an idealized problem: the two-dimensional flow of a magnetized plasma moving above an insulating surface. This analysis can be used to understand the physics of magnetoplasmadynamic (MPD) thrusters such as the system considered by Di Capua and Jahn[6] and shown in Fig. 1.

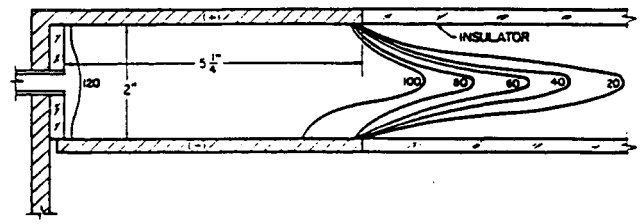

Fig. 1 Geometry of the experiment of Di Capua and Jahn.[6]

The definition of the problem is the following: The magnetic field is oriented in the z direction. The plasma flows in the region $y > 0$. The boundary, located at $y = 0$, is a perfect conductor for $x < 0$ and an insulator for $x > 0$. At large distances from this boundary the plasma velocity is parallel to $y = 0$ and is oriented towards $x = +\infty$. The analysis is based on a simple one-fluid MHD model with constant transport coefficients. It is assumed that the Reynolds and the magnetic-Reynolds numbers are large. In addition to the classical viscous and thermal boundary layers, a magnetic boundary layer develops near the insulating surface. Strong electric currents appear in this boundary layer. Ohmic heating releases the electromagnetic energy convected by the plasma leading to an increase of its temperature.

The traditional approach to the analysis of compressible boundary layers is to find a similarity transformation derived from the Illingworth-Stewartson transformation, which turns the boundary-layer equations into a variation of the Blasius equation. A different approach is taken here. It consists of applying a simple geometric transformation to the coordinates and solving the resulting system of ordinary differential equations with a numerical solver. The results show that the conversion of the electromagnetic energy into thermal energy leads to high temperatures and heat transfer rates near the insulator surface, and that under certain conditions the boundary layer draws the flow towards the insulating surface.

II. Formulation

In Cartesian coordinates the equations can be written

$$\frac{\partial}{\partial \bar{x}}(\bar{\rho}\bar{u}) + \frac{\partial}{\partial \bar{y}}(\bar{\rho}\bar{v}) = 0 \tag{1}$$

$$\bar{\rho}\bar{u}\frac{\partial \bar{u}}{\partial \bar{x}} + \bar{\rho}\bar{v}\frac{\partial \bar{u}}{\partial \bar{y}} + \frac{\partial}{\partial \bar{x}}\left(\bar{P} + \frac{\bar{B}^2}{2\mu_0}\right) = \frac{\partial}{\partial \bar{x}}\left(2\mu\frac{\partial \bar{u}}{\partial \bar{x}} + \lambda \operatorname{div} \bar{v}\right) + \mu\frac{\partial}{\partial \bar{y}}\left(\frac{\partial \bar{u}}{\partial \bar{y}} + \frac{\partial \bar{v}}{\partial \bar{x}}\right) \tag{2}$$

$$\bar{\rho}\bar{u}\frac{\partial \bar{v}}{\partial \bar{x}} + \bar{\rho}\bar{v}\frac{\partial \bar{v}}{\partial \bar{y}} + \frac{\partial}{\partial \bar{y}}\left(\bar{P} + \frac{\bar{B}^2}{2\mu_0}\right) = \mu\frac{\partial}{\partial \bar{x}}\left(\frac{\partial \bar{u}}{\partial \bar{y}} + \frac{\partial \bar{v}}{\partial \bar{x}}\right) + \frac{\partial}{\partial \bar{y}}\left(2\mu\frac{\partial \bar{v}}{\partial \bar{y}} + \lambda \operatorname{div} \bar{v}\right) \tag{3}$$

$$\frac{1}{\gamma - 1}\bar{\rho}^{\gamma}\left(\bar{u}\frac{\partial}{\partial \bar{x}} + \bar{v}\frac{\partial}{\partial \bar{y}}\right)\left(\frac{\bar{T}}{\bar{\rho}^{\gamma-1}}\right) = \frac{1}{\sigma\mu_0^2}\left[\left(\frac{\partial \bar{B}}{\partial \bar{x}}\right)^2 + \left(\frac{\partial \bar{B}}{\partial \bar{y}}\right)^2\right] + \lambda(\operatorname{div} \bar{v})^2 + k\left(\frac{\partial^2 \bar{T}}{\partial \bar{x}^2} + \frac{\partial^2 \bar{T}}{\partial \bar{y}^2}\right) + \mu\left[2\left(\frac{\partial \bar{u}}{\partial \bar{x}}\right)^2 + 2\left(\frac{\partial \bar{v}}{\partial \bar{y}}\right)^2 + \left(\frac{\partial \bar{u}}{\partial \bar{y}} + \frac{\partial \bar{v}}{\partial \bar{x}}\right)^2\right] \tag{4}$$

$$\bar{\rho}\bar{u}\frac{\partial}{\partial \bar{x}}\left(\frac{\bar{B}}{\bar{\rho}}\right) + \bar{\rho}\bar{v}\frac{\partial}{\partial \bar{y}}\left(\frac{\bar{B}}{\bar{\rho}}\right) = \frac{1}{\sigma\mu_0}\left(\frac{\partial^2 \bar{B}}{\partial \bar{x}^2} + \frac{\partial^2 \bar{B}}{\partial \bar{y}^2}\right) \tag{5}$$

Received March 10, 1993; revision received Feb. 9, 1994; accepted for publication Feb. 14, 1994. Copyright © 1994 by the American Institute of Aeronautics and Astronautics, Inc. All rights reserved.

*Research Assistant, Department of Aeronautics and Astronautics.

The dependent variables: $\bar{\rho}$, $\bar{v}$, $\bar{P}$, $\bar{T}$, $\bar{B}$ represent, respectively: the density, velocity, pressure, temperature, and the component of the magnetic field in the e_z direction. The transport coefficients are σ for electric conductivity, λ and μ for viscosity, and k for heat conductivity. The coefficient μ_0 stands for the magnetic permittivity of vacuum.

The variables are scaled by their reference values: $\bar{\rho}_0$, $\bar{u}_0$, $\bar{P}_0$, $\bar{T}_0$, $\bar{B}_0$, $\bar{L}_0$. The reference length scale is chosen equal to $\Lambda_m = (\mu_0\sigma\bar{u}_0)^{-1}$. This is the length scale at which the diffusive effects balance the convective effects in the magnetic field equation. The conditions at large distances can be used to define an intrinsic Mach number and an intrinsic Mach-Alfven number, respectively, equal to

$$M_a^2 = \frac{\bar{\rho}_0\bar{u}_0^2}{\gamma\bar{P}_0} \quad \text{and} \quad M_v^2 = \frac{\mu_0\bar{\rho}\bar{u}_0^2}{\gamma\mu_0\bar{P}_0 + \bar{B}_0^2}$$

In order to leave M_a and M_v invariant the reference variables are required to satisfy

$$(\bar{B}_0^2/2\mu_0) = \bar{P}_0 = \bar{\rho}_0\bar{u}_0^2$$

Two reference variables are chosen arbitrarily

$$\bar{u}_0 = \lim_{\bar{y}\to\infty} \bar{u} \quad \text{and} \quad \bar{\rho}_0 = \lim_{\bar{y}\to\infty} \bar{\rho}$$

The other reference variables are derived from the definition of M_a and M_v.

The nondimensionalization of the equations introduces two independent nondimensional numbers related to the momentum and heat transfer phenomena. The following numbers were chosen: the Prandtl number, $P_r = C_p\mu/k$, and the equivalent of the Prandtl number for the magnetic diffusion, $P_m = \sigma\mu_0\mu/\rho_0$. The transport coefficients σ, λ, μ are considered constant across the boundary layer.

To transform the problem into a self-similar problem the first step is to rescale the variables by the following transformations: $x = (X/\varepsilon)$, $y = (Y/\sqrt{\varepsilon})$, and

$$(\rho, u, v, t, p, b) = (R, U, \varepsilon^{1/2}V, T, P, B) + \cdots$$

where x, y, ρ, u, v, t, p, b are the nondimensional variables, and $\varepsilon \to 0$. This leads to a set of boundary-layer equations. The second step is to find a similarity transformation that turns these equations into a system of ordinary differential equations. For a flat plate, one can use the following transformation where the independent variables become $\eta = (Y/\sqrt{X})$, $\xi = X$, and the dependent variables take the form: $R = R(\eta)$, $U = U(\eta)$, $V = \xi^{-1/2}W(\eta)$, $T = T(\eta)$, $P = P(\eta)$, and $B = B(\eta)$. Substituting the new variables and keeping the terms of dominant order in ξ, leads to a system of ordinary differential equations

$$-\frac{1}{2}\eta\frac{\partial}{\partial\eta}(RU) + \frac{\partial}{\partial\eta}(RW) = 0 \tag{6}$$

$$R\left(W - \frac{1}{2}\eta U\right)\frac{\partial U}{\partial\eta} - \frac{1}{2}\eta\frac{\partial}{\partial\eta}(RT + B^2) = P_m\frac{\partial^2 U}{\partial\eta^2} \tag{7}$$

$$\frac{\partial}{\partial\eta}(RT + B^2) = 0 \tag{8}$$

$$\frac{1}{\gamma - 1}R^\gamma\left(W - \frac{1}{2}\eta U\right)\frac{\partial}{\partial\eta}\left(\frac{T}{R^{\gamma-1}}\right) = 2\left(\frac{\partial B}{\partial\eta}\right)^2 + P_m\left[\frac{\gamma}{\gamma - 1}\frac{1}{P_r}\frac{\partial^2 T}{\partial\eta^2} + \left(\frac{\partial U}{\partial\eta}\right)^2\right] \tag{9}$$

$$R\left(W - \frac{1}{2}\eta U\right)\frac{\partial}{\partial\eta}\left(\frac{B}{R}\right) = \frac{\partial^2 B}{\partial\eta^2} \tag{10}$$

with the following boundary conditions: $R(\infty) = \rho_e$, $U(\infty) = u_e$, $T(\infty) = T_e$, $B(\infty) = b_e$, $U(0) = 0$, $W(0) = 0$, $B(0) = 0$. For the temperature condition at the wall, one can define either a "cold" wall condition: $T(0) = T_0$, or an insulated wall condition: $(\partial T/\partial Y)_0 = 0$. The system of ordinary differential equations is integrated numerically with the package called COLNEW written by Ascher et al.[7]

III. Discussion

The results for the "cold wall" condition are shown in Fig. 2. The parameters for this calculation are $M_a = 3.323$, $M_v = 1$, $P_r = 1$, and $P_m = 0.001$. In this figure the horizontal coordinate is η and the vertical coordinate represents the values of the density R, the longitudinal velocity U, the magnetic field B, the pressure P, the normal velocity W, and the temperature T.

The results indicate the existence of a strong heat transfer near the wall. As the viscous and thermal diffusion decrease relative to the magnetic diffusion, the thermal effects become more pronounced. In the cold wall problem this means that the heat flux increases as the Reynolds number goes to infinity. In the "insulating wall" problem this means that the wall temperature increases.

For certain values of the parameters, the boundary layer draws the fluid towards the wall. Once the fluid has penetrated

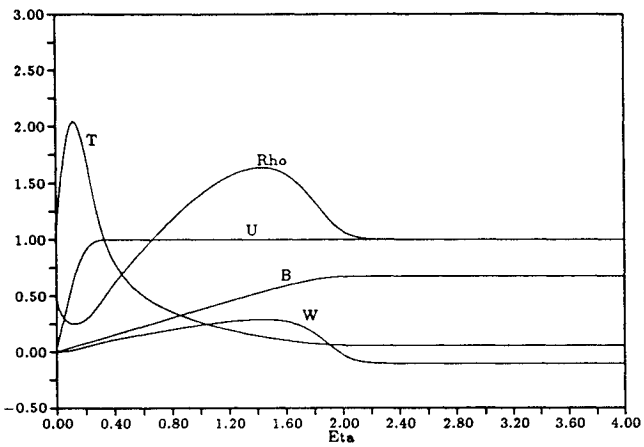

Fig. 2 Boundary layer over a flat insulator for the cold wall condition.

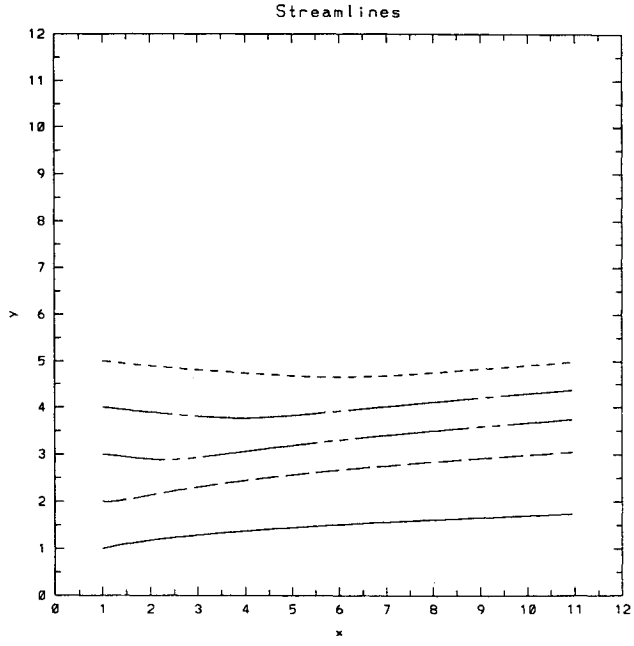

Fig. 3 Streamlines above an insulator plate.

inside the boundary layer the direction of the normal velocity changes and the fluid moves away from the wall. This phenomenon is visible in Fig. 3, which shows a few streamlines. The viscous and thermal diffusion must be small for this phenomenon to appear. In other words the magnetic Prandtl number P_m must be lower than a critical value P_m^*. For an insulating wall this critical value falls in the interval (0.002, 0.005). For a cold wall it falls in the interval (0.03, 0.1) when $T_{(0)} = 1$. Both results are for the conditions $M_a = 3.323$, $M_v = 1$, $P_r = 1$.

In addition, the density shows a maximum in the middle of the boundary layer. This can be explained in the following way: As the fluid moves into the boundary layer it first undergoes an adiabatic compression under the influence of the magnetic pressure. (This can be seen by looking at the direction of the Lorentz force: $\boldsymbol{f} = \boldsymbol{j} \times \boldsymbol{b}$.) Thus, as the magnetic field decreases, the gas pressure rises. This adiabatic compression leads to an increase in the density, $\rho \sim p^{0.6}$, and in the temperature: $t \sim p^{0.4}$. As the gas penetrates inside the boundary layer the Ohmic heat release becomes significant and the compression is no longer isentropic. The temperature t increases under the influence of the Ohmic dissipation as well as the viscous friction. Since the pressure is approximately constant, the density decreases. Next to the wall the heat diffusion balances the heat generation (Ohmic and viscous friction), and the density may either increase or decrease depending on the type of boundary condition considered.

Experimental results that could be used to check the predictions of this analysis are difficult to find. The current distribution for the parallel-plate thruster tested by Di Capua and Jahn[6] is shown in Fig. 1, but other variables were not reported.

IV. Conclusions

It has been shown that the presence of insulating surfaces downstream of a plasma containing a residual magnetic field will give rise to very intense local heating along the surface of the insulator. This heating is the result of the recovery of the gas kinetic energy released by viscous friction, as well as the recovery of the residual electromagnetic energy released by Ohmic heating. At high values of the magnetic Reynolds number the flow is drawn towards the insulators and the density reaches a maximum in the middle of the boundary layer.

This article also proposes a new similarity method to solve boundary-layer problems. This method was applied to a compressible magnetodynamic boundary layer, but can also be applied to many boundary-layer problems traditionally studied using the Illingworth-Stewartson transformation.

References

[1]Wilcox, M. W., "The Magnetofluiddynamical Viscous Compressible Flow About Wedges and Flat Plates," *Proceedings of the 4th Biennial Gas Dynamics Symposium*, edited by A. B. Cambel, T. P. Anderson, and M. M. Slawsky, Northwestern Univ. Press, Evanston, IL, 1962, pp. 277–298.

[2]Fay, J. A., "Plasma Boundary Layers," *Proceedings of the 4th Biennial Gas Dynamics Symposium*, edited by A. B. Cambel, T. P. Anderson, and M. M. Slawsky, Northwestern Univ. Press, Evanston, IL, 1962, pp. 337–348.

[3]Moffat, W. C., "Approximate Solutions for the Skin Friction and Heat Transfer in MHD Channel Flows," Project Squid Technical Rept., MIT-36-P, Cambridge, MA, June 1965.

[4]Daily, J. W., Kruger, C. H., Self, S. A., and Eustis, R. H., "Boundary Layer Profile Measurements in a Combustion Driven MHD Generator," *6th International Conference on Magnetohydrodynamic Electrical Power Generation*, Vol. 1 (Washington, DC), National Technical Information Services, Springfield, VA, 1975, pp. 451–463.

[5]Pai, S. I., *Magnetogasdynamics and Plasma Dynamics*, Springer-Verlag, Vienna, Austria, 1963, pp. 67, 68.

[6]Di Capua, M. S., and Jahn, R. G., "Energy Deposition in Parallel-Plate Plasma Accelerators," AIAA Paper 71-197, Jan. 1971.

[7]Ascher, U. M., Mattheij, R. M. M., and Russel, R. D., *Numerical Solution of Boundary Value Problems for Ordinary Differential Equations*, Prentice Hall, Englewood Cliffs, NJ, 1988, pp. 526–533.

Unsteady Heat Transfer from a Thick Hot-Film Sensor

Chong H. Park* and Kevin D. Cole†
University of Nebraska at Lincoln, Lincoln, Nebraska 68588

Introduction

METAL-FILM sensors have been widely used as temperature sensors, heat flux sensors, shear-stress sensors, and recently as separation detectors. In all of these applications, the thermal storage in the sensor can be neglected if the metal film is "thin." Schultz and Jones[1] indicate that the thermal storage in the sensor may be neglected for heat flux sensors in a flow containing frequencies below 10 kHz if the metal film is less than 0.1 μm. However, the sensor studied in this Note has a thick metal film with thickness e of 6 μm on a polymer substrate that is glued to a surface for use in an airflow. The advantage of a thick-metal sensor is that it can carry more electric current, and therefore gives a higher output voltage. The present research is to develop numerical and analytical models of the thick sensor that include thermal storage in the sensor.

Transient conjugate heat transfer analysis is carried out with the unsteady surface element (USE) method. The USE method is a boundary discretization method and is a very efficient method for solving conjugate heat transfer problems.[2] In this Note, the temperature response of the sensor is determined from analysis of three bodies (air, hot film, and polymer substrate). The average temperature of the hot-film sensor is determined, with known heat flux input to the hot film and with known air velocity. The present work that involves steady airflow with transient heat transfer is a first step toward transient airflow analysis of these sensors.

Boundary Value Problem

Figure 1 shows the geometry of the conjugate heat transfer problem. The two-dimensional geometry applied here is appropriate for the large aspect ratio ($b/a = 85$) hot-film sensor. Refer to Park and Cole[3] for the actual configuration for hot-film sensors provided by Pratt & Whitney United Technologies. The parameters a and b are streamwise and spanwise half-length of the hot film, respectively. All material properties are treated as constant values (small temperature rise assumed). A single-layer substrate with an effective thickness D is used to represent the actual multiple-layered solid composed of a polymer layer, glue layer, and the underlying metal surface to which the sensor is glued. For airflow, radiation and natural convection are neglected, viscous dissipation is neglected, and the streamwise conduction in the flow is neglected. The airflow has a linear velocity profile ($u = \beta y_f$). Although the hot film is thermally thick, it is mechanically so small that it does not disturb the airflow.

Received Oct. 25, 1993; revision received Feb. 22, 1994; accepted for publication Feb. 25, 1994. Copyright © 1994 by the American Institute of Aeronautics and Astronautics, Inc. All rights reserved.

*Instructor, Mechanical Engineering Department.

†Associate Professor, Mechanical Engineering Department. Member AIAA.